Colloid Polym Sci (2005) 283: 383–392
DOI 10.1007/s00396-004-1157-5

ORIGINAL CONTRIBUTION

Shouhong Xu
Yuan Song
Shizuko Sato
Isamu Miyata
Junpei Yamanaka
Masakatsu Yonese

Surface structures of adsorption layers of sodium hyaluronate and bovine serum albumin complexes on poly(γ-methyl-L-glutamate) film and their surface properties

Received: 18 December 2003
Accepted: 15 April 2004
Published online: 23 June 2004
© Springer-Verlag 2004

S. Xu (✉) · Y. Song · S. Sato · I. Miyata
J. Yamanaka · M. Yonese
Graduate School of Pharmaceutical Sciences, Nagoya City University,
467-8603 Tanabe-dori Mizuho-ku
Nagoya, Japan
E-mail: xushou@yahoo.co.jp
Fax: +81-52-8363443

Abstract Two-dimensional structures and characteristics of the complexes between sodium hyaluronate (NaHA) and bovine serum albumin (BSA) were studied by using a quartz crystal microbalance method and an atomic force microscope (AFM). NaHA did not adsorb on poly(γ-methyl-L-glutamate) (PMLG) film. On the other hand, the complexes adsorbed on it and the adsorption behaviors were found to be Langmuir types. With increasing weight ratio of BSA to NaHA, W_{BSA}, the adsorption constants K decreased and the saturated adsorption masses Γ^{∞} increased. The adsorbed complexes were spherical particles and at saturated adsorption states they covered compactly on the PMLG film. The mean diameters d_{AFM} estimated from the topographic images decreased from 70 to 54 nm with increasing W_{BSA}. The adhesion force F_{ad} and the frictional force F_f between the complex layers and the AFM tip were obtained by using the contact mode of the AFM. With increasing W_{BSA}, the values of F_{ad} decreased and the values of F_f increased. Compared with the frictional coefficient of the NaHA adsorption layer on the BSA monolayer, the values for the NaHA–BSA complex layer were found to be much higher.

Keywords Sodium hyaluronate · Atomic force microscope · Two-dimensional nanostructure · Adhesion force · Frictional force

Introduction

Acid mucopolysaccharides are widely distributed in living tissues, such as skin, cartilage, joints and glass body fluids. They are negatively charged linear polysaccharides and possess carboxylic and/or sulfuric groups. They do not only exist alone but also combine with collagen as proteoglycans, and function as the main component of extracellular matrixes [1]. They have been studied biologically and physicochemically, and their molar masses and the arrangements of the charged groups are closely related to biofunctions and aging. Hyaluronate (HA), being one of the acid mucopolysaccharides, is composed of repeating disaccharides units, D-glucuronate and *N*-acetyl-D-glucosamine, and possesses one carboxylic group per repeating unit [2, 3, 4]. In solutions, it is known that HA has a helical structure and above the overlap concentration forms a network structure. The resultant high viscoelasticity has an important role in the synovial fluid of a joint [5, 6]. The molar masses of HA are reported to decrease owing to aging and diseases such as arthritis. Complex formations of HA with proteins and their phase separations are also related to the biofunctions. They have been studied basically as coacervates. We consider that the properties of HA and the complexes at interfaces are very important as well as in solutions to elucidate the

biofunctions, such as the mechanism of low friction at the interface of cartilage [7] and of a cataract [8, 9].

Complex formations due to electrostatic interactions between oppositely charged polymers are affected by pH, the ion strength and the concentration of the solutions. According to Kokufuta and Dubin [10] the complexes are grouped into intrapolymer and interpolymer complexes: the former is a soluble complex; the latter is formed by the bindings between the intrapolymer complexes and brings about a phase separation. Since the complexes were found to form nanoparticles, they have attracted attention from not only basic but also applied points of view in pharmaceutical and technological fields [11, 12, 13]. The nanoparticles were reported to act as unique hosts for macromolecular guests, such as enzymes or other proteins, and to improve the stability of the denaturation of proteins [14, 15]. HA and proteins form soluble complexes in the neutral or the weakly acidic pH region, and in the more acidic pH region phase separation occurs. We have studied the features of complexes composed of sodium hyaluronate (NaHA) and bovine serum albumin (BSA) in solutions and their sizes were found to be controlled by the composition, i.e., the complexes shrunk with increasing BSA and formed particles several 100 nm in diameter [16, 17].

On the other hand, polymers at an interface have been noted recently in biotechnology and nanotechnology. Relations between the interfacial structure and the function have been studied using a layer-by-layer method and the Langmuir–Blodgett method [18]. We have studied autoorganized interfacial nanostructures of NaHA formed by the layer-by-layer method and their interfacial properties [19, 20]. It was found that the adsorptions of NaHA on a BSA monolayer were of the Langumir type and the structures were honeycomb-like networks. The structures and the properties are affected by the molar masses of NaHA M_w. With decreasing M_w, the mesh size increased and the frictional coefficients increased.

In this work, we studied the interfacial adsorption mechanisms, the structures and the properties of NaHA–BSA complexes using a quartz crystal microbalance (QCM) and an atomic force microscope (AFM). The AFM was used not only to obtain morphological images of the surfaces, but also to investigate the nanomechanical properties, such as the adhesion force F_{ad} and the frictional force F_f. From lateral force measurements, F_f was obtained and the frictional coefficient μ was estimated.

Experimental

Materials

NaHA obtained from Seikagaku Kogyo Co. was used without any purification. The average molar mass M_w was determined to be 8.50×10^5 g mol^{-1} (composed of 2,120 repeating units) using static light scattering (Otsuka Electronics Co., DLS–700Ar). BSA was purified by delipidizing a BSA fraction V (Seikagaku Kougyou) as follows. (1) To the BSA solution (10 w/v %, 100 cm^3), activated carbon (5 g, Darco Co., G-60) was added. (2) After adjusting the solution to pH 3, the solution was stirred in an ice bath for 2 h, and then centrifuged under 24,000*g* for 30 min. (3) The supernatant was filtered and adjusted to pH 5 by adding NaOH (0.2 mol dm^{-3}). (4) The solution was passed through a mixed column (cation-exchange resin/anion-exchange resin 1:1) and then freeze-dried. The cation-exchange and anion-exchange resins were of Amberlite IR 120B and IRA 400 (Organo Co.) [17]. The value of M_w of BSA was determined to be 7.0×10^4 g mol^{-1} by using static light scattering (Otsuka Electronics Co., DLS-700Ar). The isoelectric point of BSA was 5.2. Poly(γ-methyl-L-glutamate) (PMLG, Sigma Co., $M_w = 307{,}000$ g mol^{-1}) was of a commercial origin and was used without any purification. 1,2-Dichloroethane used as the solvent of PMLG was a special grade (Wako Co.) and other reagents were also all special grades (Katayama Co.). Water was distilled and deionized.

Preparation of the PMLG tip of the QCM

A PMLG solution was prepared by dissolving 10 mg PMLG in 10 ml 1,2-dichloroethane and was cast on the disk tip of the QCM (USI System Co., Japan). Since the β-sheet form of PMLG does not dissolve in 1,2-dichloroethane [21], the PMLG solutions were used as a casting solution after filtrating through the filter (pore size 0.5 μm, Millipore Co.). PMLG films were prepared by spreading the casting solution (2 μl) on both sides of the QCM disk tips. The area of each surface was 1.59×10^{-1} cm^2, where Au was deposited by evaporation. After drying in a desiccator at room temperature, the cast mass of PMLG on both sides of the tip was determined to be 1.4 μg (4.5×10^{-12} mol) from the changes of the resonance frequency of the QCM. The tip is denoted by the PMLG tip.

Measurement of adsorption masses on PMLG film in NaHA–BSA complex solutions by the QCM

Four kinds of complex solutions were prepared by adding various amounts of BSA ($C_{BSA} = 2.0$, 4.0, 6.0, 9.0×10^{-3} kg dm^{-3}) to a NaHA solution ($C_{NaHA} = 1.0\times10^{-3}$ kg dm^{-3}) under a constant ionic strength adjusted by NaCl ($J = 0.001$ mol dm^{-3}). Their weight ratios of BSA to NaHA W_{BSA} were 2, 4, 6 and 9, and their total weight concentrations of the solutions C_T were 3.0, 5.0, 7.0, 10.0×10^{-3} kg dm^{-3}. On measuring the adsorption masses in the complex solutions, the four

original complex solutions were diluted by 50, 100, 200, 500 times respectively. Their pH values were almost 5.8 near the isoelectric point of BSA. The PMLG tip was immersed into them at 25 °C. The solutions were gently stirred in order to deprive the effect of the unstirred layer as much as possible without losing the stability of the QCM frequency. The adsorption masses were obtained from the decrease of the resonance frequency of the QCM tip Δf. The resonance frequency of the QCM tip was 9 MHz. According to Sauerbrey's equation [22, 23], a frequency decrease of 1 Hz corresponded to a mass increase of 0.87 ng on the QCM tip.

Observation of surface structures of NaHA–BSA complexes on the PMLG film by AFM

After drying the adsorption layer on the PMLG tip in a desiccator at room temperature, the surface structures were observed by using the tapping mode of the AFM (Nanoscope III, Digital Instruments Co., USA) in air. An AFM tip made of a silicone monocrystal (type NCH-W, normal spring constant $K_N = 33$ N m^{-1}, Digital Instruments Co.) was used without any surface treatment. Topographic images were captured and three-dimensional information on the particles were obtained simultaneously by using off-line analysis.

Measurement of adhesion force F_{ad} between the NaHA–BSA complex layer and the AFM tip

The adhesion forces F_{ad} between the adsorption layers and the AFM tip were measured in the equilibrated complex solutions by the contact mode of the AFM. To protect the electronics of the AFM from the solution, a Teflon skirt was placed above the cantilever. F_{ad} is equal to the pull-off force of the tip from a surface and can be given directly from a force–distance curve. The values of F_{ad} were measured at various vertical positions of the tip. The tip for the contact mode was also made of the silicone monocrystal and the value of K_N calibrated by the manufacturer was 0.13 N m^{-1}. It was softer than that used in the tapping mode to get more accurate data and to cause less damage to the sample surface.

Measurement of frictional force F_f between the NaHA–BSA complex layer and the AFM tip

The frictional forces F_f between the adsorption layers and the AFM tip were measured in the equilibrated complex solutions using a lateral force microscope, and were measured in the contact mode at a scanning angle of 90° as reported in a previous paper [19, 20]. The tip was scanned in the lateral direction to obtain the torsions in the trace and the retrace. The torsions of the tip were measured under several load forces F_{load} exerted by changing a set point of the tip. The difference of the torsions between the trace and the retrace was twice as much as F_f. From the value of F_f, the frictional coefficient μ can be obtained from Eq. (1),

$$F_f = \mu(F_{load} + F_{ad}). \quad (1)$$

The scanning area was 2.0 μm×2.0 μm, which was smaller than the areas of the AFM images (2.5 μm×2.5 μm).

Results

Adsorptions of NaHA and the NaHA–BSA complex on PMLG film

The adsorptions of NaHA and the NaHA–BSA complex on the PMLG film were measured using the QCM method by immersing the PMLG tip into their solutions of various concentrations. The adsorption masses Γ were obtained from the decreases of the resonance frequency Δf of the PMLG tip. The values of Γ in the NaHA solutions were almost zero in the concentration region $C_{NaHA} = 0.1\times10^{-5}$-$2.0\times10^{-5}$ kg dm^{-3}. The results for the most concentrated solution are shown in Fig. 1 by filled circles as a function of time t. Although NaHA molecules did not adsorb on the PMLG film, in NaHA–BSA complex solutions adsorptions were found. As typical results, Fig. 1 shows the time courses of Γ in the complex solutions with $W_{BSA} = 9$. Their concentrations were in the region $C_T = 1.0\times10^{-5}$–20×10^{-5} kg dm^{-3}. Within 10 min, the adsorptions attained equilibrium. The equilibrium adsorption masses are shown in Fig. 2 as a function of C_T together with the results for other complex solutions. They showed Langmuir-type adsorptions and the saturated adsorption masses Γ^{∞} increased with increasing W_{BSA}.

The adsorptions were analyzed by the Langmuir adsorption isotherm [1]. Their reciprocal plots were linear as shown in Fig. 3 and their adsorptions were confirmed to be of the Langmuir type. The values of the adsorption constant K and Γ^{∞} were obtained from the slope and the intercept. They are summarized in Table 1 as well as the results for BSA [1]. With increasing W_{BSA}, K decreased and Γ^{∞} increased. The solid curves in Fig. 2 show the fitting results which were calculated using these parameters.

Topographic images of the QCM and PMLG tips

Topographic images of the Au surface layer of the QCM tip and the PMLG film on the Au layer (PMLG tip) were observed using the tapping mode of the AFM in air. As shown in Fig. 4, the Au layer was made up of

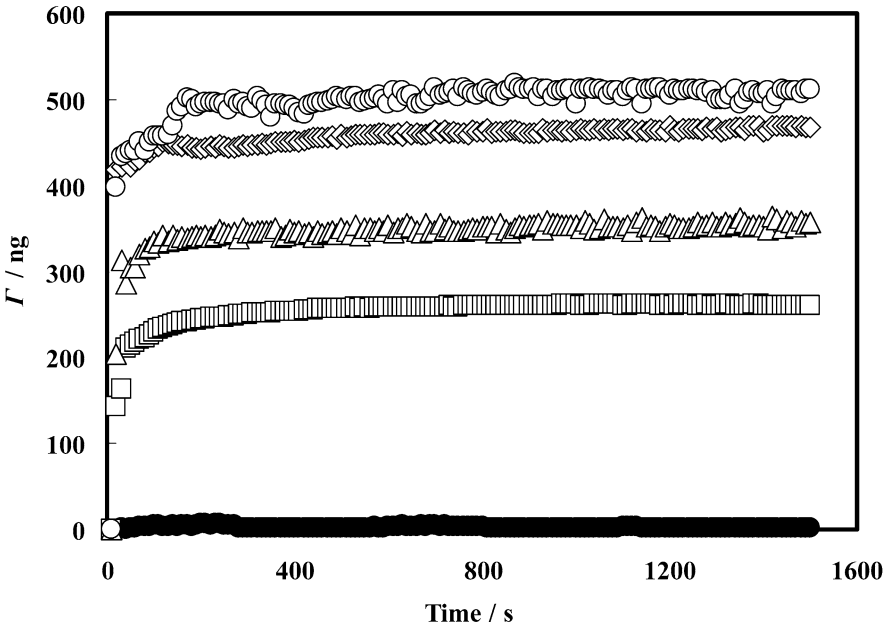

Fig. 1 Time courses of adsorption masses on poly(γ-methyl-L-glutamate) (*PMLG*) film in sodium hyaluronate (*NaHA*) and NaHA–bovine serum albumin (*BSA*) complex solutions (weight ratio of BSA to NaHA $W_{BSA} = 9$). NaHA solution: $C_{NaHA} = 2.0\times10^{-5}$ kg dm^{-3} (*filled circles*). Complex solutions: $C_T = 1.0\times10^{-5}$ kg dm^{-3} (*squares*); $C_T = 5.0\times10^{-5}$ kg dm^{-3} (*triangles*); $C_T = 10\times10^{-5}$ kg dm^{-3} (*diamonds*); $C_T = 20\times10^{-5}$ kg dm^{-3} (*open circles*)

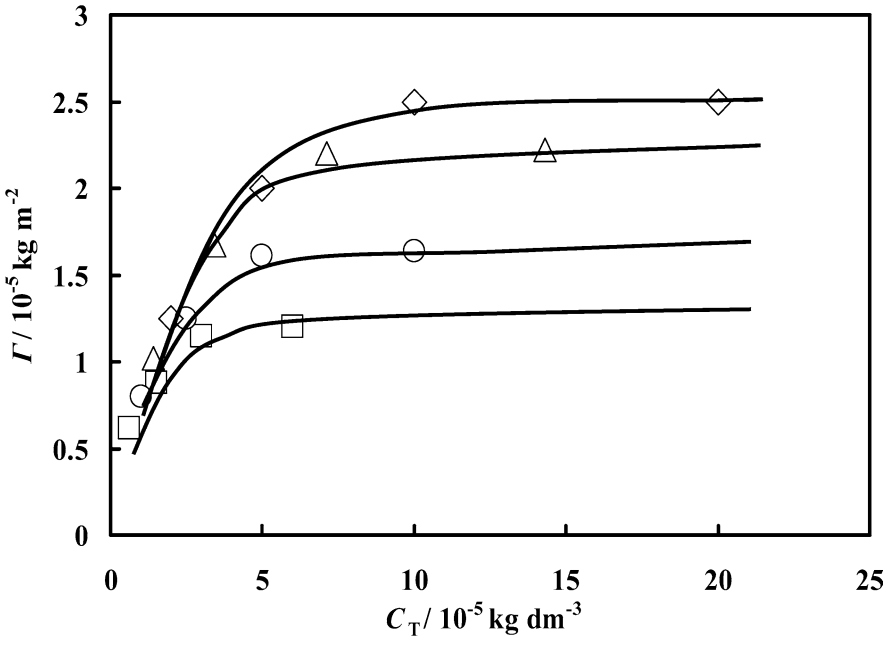

Fig. 2 Adsorption masses on PMLG film Γ of the NaHA–BSA complex as a function of total weight concentration of the solutions C_T. The weight ratio of BSA to NaHA in solution $W_{BSA} = 2$ (*squares*), $W_{BSA} = 4$ (*circles*), $W_{BSA} = 6$ (*triangles*), $W_{BSA} = 9$ (*diamonds*)

spherical particles 125 ± 10 nm in diameter. The PMLG film gave almost the same image as the Au layer and the mean diameter increased slightly to become 140 ± 10 nm. The PMLG film was considered to cover uniformly multilayer states. The area of α-helix PMLG was reported to be 0.175 nm^2 per residue and the diameter of the cross section to be 1 nm [21]. From the value of Γ of PMLG (1.4 μg, 4.5×10^{-12} mol) on the Au layer, it was estimated that the PMLG film consists of 29 layers and that the thickness is 29 nm.

Topographic images of adsorption layers in NaHA–BSA complex solutions

The adsorption layers on the PMLG film were observed using the tapping mode in the same manner as previously. The topographic images of the adsorption layers in the complex solution of $W_{BSA} = 9$ under various adsorption states are shown in Fig. 5. We found spherelike particles increasing in number and decreasing slightly in size with increasing degrees of

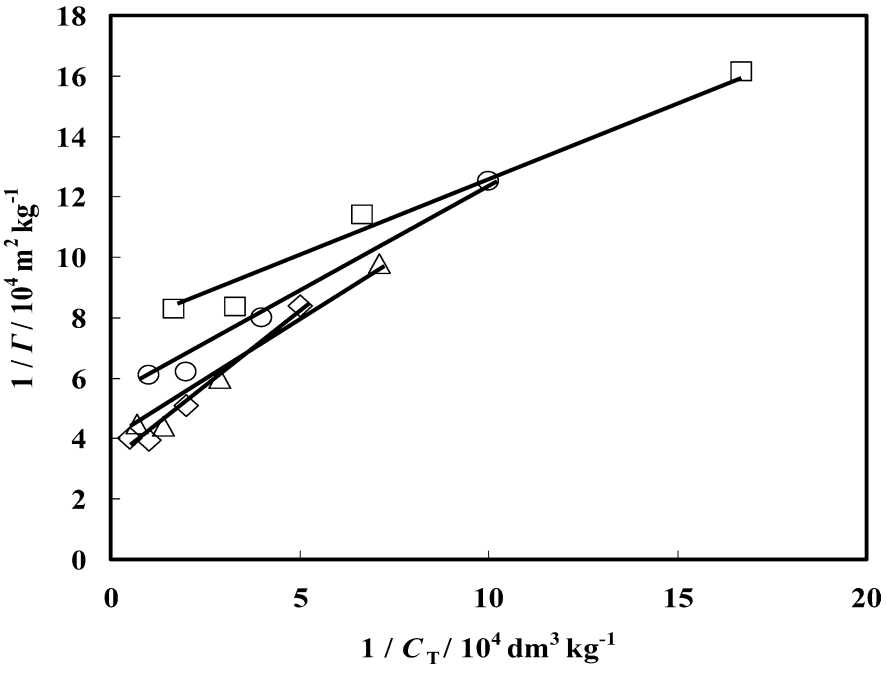

Fig. 3 Reciprocal plot of the adsorption massΓ and weight concentration of the solution C_T. The weight ratio of BSA to NaHA in solution $W_{BSA}=2$ (*squares*), $W_{BSA}=4$ (*circles*), $W_{BSA}=6$ (*triangles*), $W_{BSA}=9$ (*diamonds*)

Table 1 Adsorption characteristics of saturated layers of bovine serum albumin (*BSA*) and sodium hyaluronate–BSA complexes. *K* is the adsorption constant and $\Gamma^{\infty}$is the saturated adsorption mass

	Composition of complex				
	$W_{BSA}=2$	$W_{BSA}=4$	$W_{BSA}=6$	$W_{BSA}=9$	BSA
$K/10^4$ dm^3 kg^{-1}	17.3	9.8	6.0	5.7	120
$\Gamma^{\infty}/10^{-5}$ kg m^2	1.25	1.67	2.3	2.5	0.27
d_H/nm	1,077	571.9	363.9	95.5	14.0
d_{AFM}/nm	70	63	57	54	38
d_{cal}/nm	17	18	18	20	7.6

occupation θ (Γ/Γ^{∞}). In the saturated adsorption as shown in Fig. 5c, the particles had an average diameter of 54 nm and were arranged compactly on the PMLG film. However, the honeycomb-like networks of NaHA [19, 20] and the smaller particles of BSA [1] reported in previous papers could not be found in the images. Then, the particles would be NaHA–BSA complexes.

The topographic images of saturated adsorption layers in various complex solutions ($W_{BSA}=2$–9) are shown in Fig. 6. Although their topographic images changed with the compositions of the solutions, spherical complex particles were observed to cover compactly on the PMLG film. The mean diameters of the complexes d_{AFM} estimated from the topographic images decreased from 70 to 54 nm with increasing W_{BSA}. The images for low W_{BSA} showed white pleats showing higher parts which were composed of strings of the complex particles. With increasing values of W_{BSA}, the pleats decreased and disappeared. It is considered to result from the change in the shape and the size of the complexes.

Three-dimensional plot of the NaHA–BSA complex

The surfaces of the PMLG film and the NaHA–BSA complex layers were observed with the same viewing and illumination angle to get three-dimensional information through an off-line analysis of the AFM. The three-dimensional plots of the PMLG film and the adsorbed complexes in the solution with $W_{BSA}=9$ in the unsaturated adsorption state ($\theta=0.6$) are shown in Fig. 7 to make clear the three-dimensional shape. The PMLG film was found to be composed of a lot of low roof domes of 140-nm mean diameter, which was almost equal to that of the topographic image. The adsorbed complex layer was found to be composed of a lot of spherelike particles. From the three-dimensional plots, the complex particles were confirmed to be spheres.

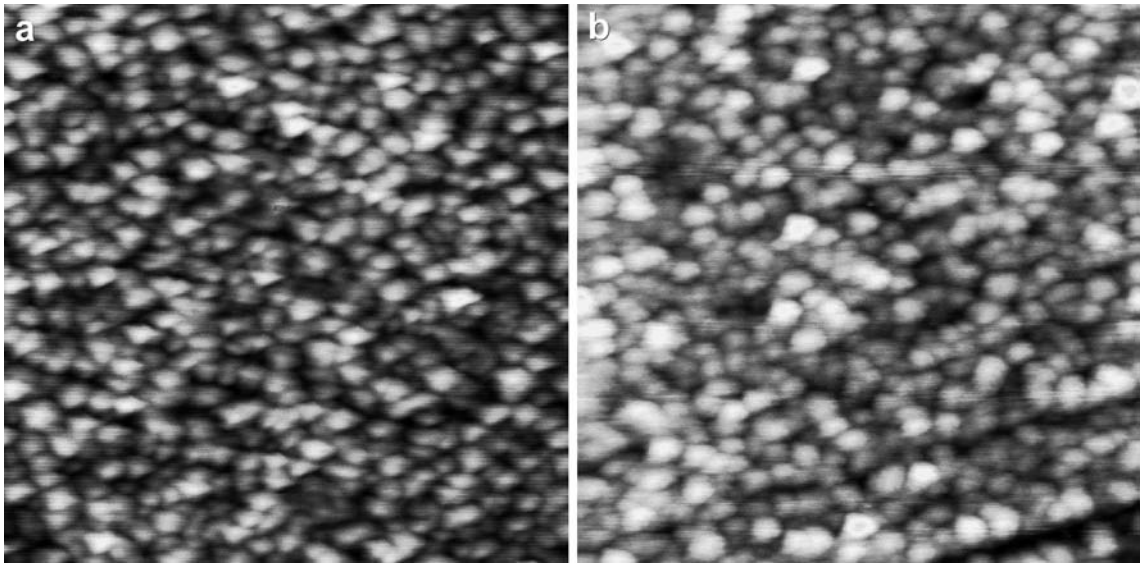

Fig. 4a,b Topographic images of an Au surface and a PMLG film observed using an atomic force microscope (*AFM*). **a** Au surface, **b** PMLG film

Adhesion force F_{ad} of NaHA–BSA complex adsorption layers

F_{ad} between the saturated adsorption layers of the NaHA–BSA complexes and the AFM tip were measured using the contact mode of the AFM in equilibrated solutions. The values of F_{ad} were obtained from the force–distance curves and were averaged from several measurements at different spots on one sample. As shown in Fig. 8, F_{ad} of the complexes decreased with increasing W_{BSA}. The F_{ad} values at $W_{BSA}=0$ are those of a PMLG film and a NaHA adsorption layer on a BSA monolayer reported in previous papers [19, 20].

Frictional force F_f of NaHA–BSA complex adsorption layers

F_f between the saturated adsorption layers of the complexes and the AFM tip were measured using a lateral force microscope in equilibrated solutions. The average values of F_f obtained at several locations as a function of F_{load} are shown in Fig. 9. The F_f values were in proportion to F_{load} and the slopes increased with increasing W_{BSA}. According to Eq. (1), the frictional coefficients μ of the complex layers were obtained from the slopes. As $F_{load} \gg F_{ad}$, F_{ad} was ignored in the calculation of μ. As shown in Fig. 10, the values of μ increased with increasing W_{BSA}. The values of μ at $W_{BSA}=0$ are those of the NaHA adsorption layers and the PMLG film.

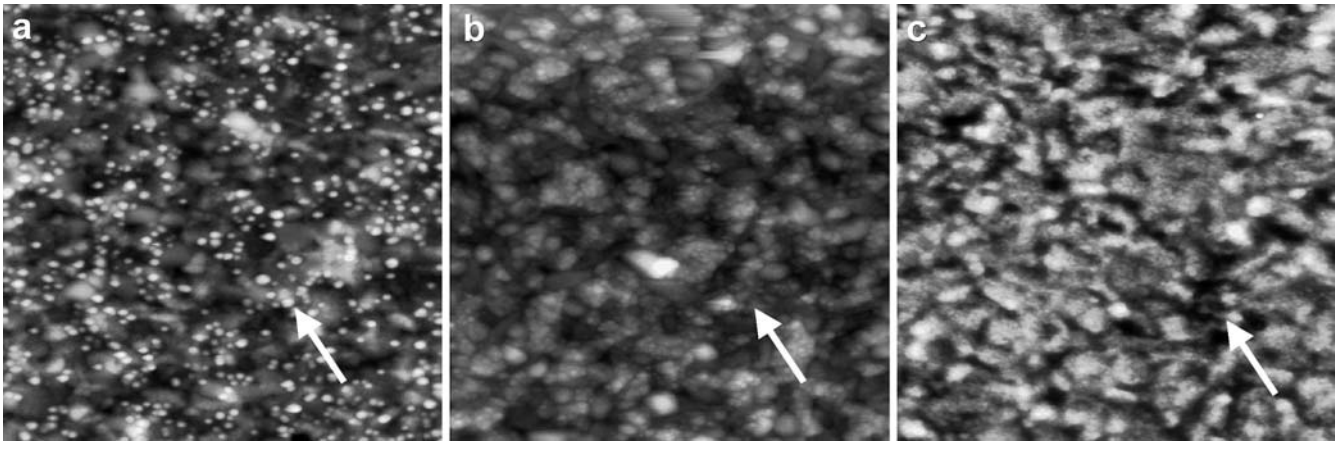

Fig. 5a–c Topographic images of the adsorption layer on a PMLG film in complex solutions of weight ratio of BSA to NaHA $W_{BSA}=9$. Degree of occupation **a** $\theta=0.6$, **b** $\theta=0.8$, **c** $\theta=1.0$. The *arrows* show the complex particle

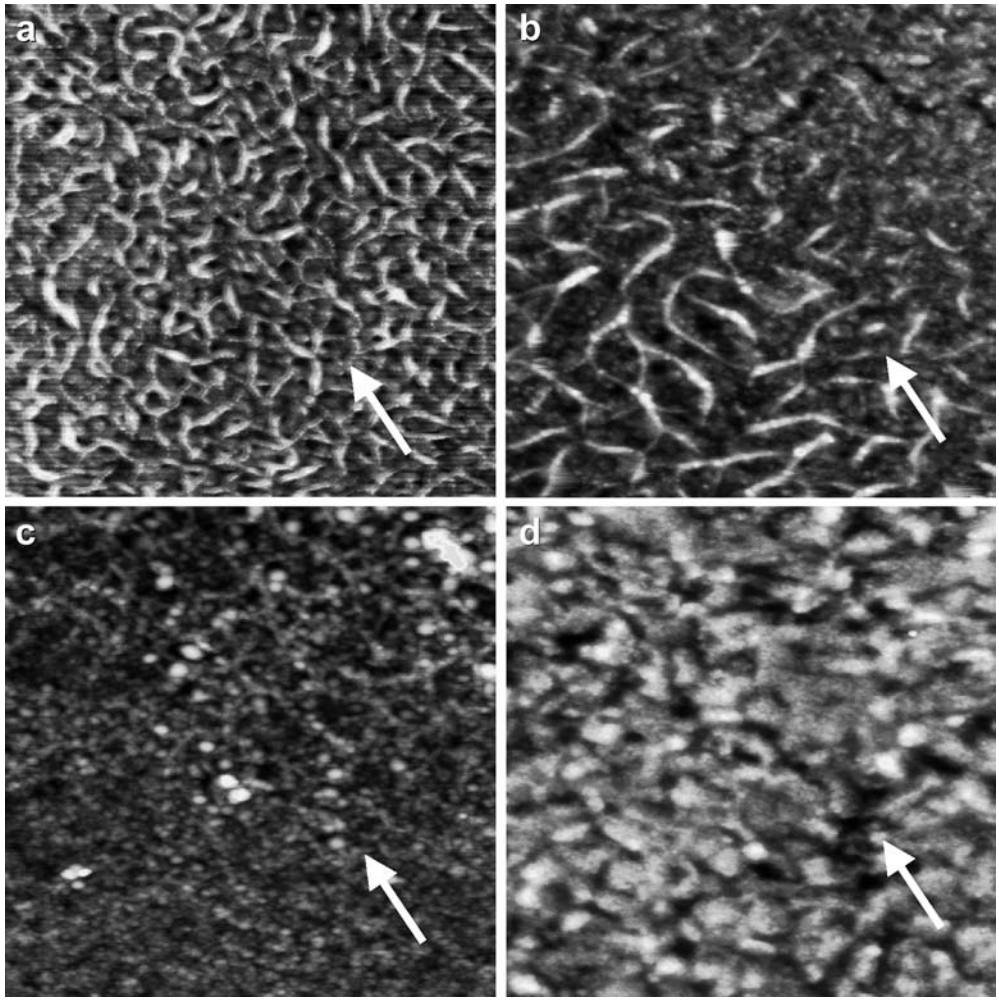

Fig. 6a–d Topographic images of saturated adsorption layers of a NaHA–BSA complex in various weight ratios of BSA to NaHA on a PMLG film. **a** $W_{BSA} = 2$, **b** $W_{BSA} = 4$, **c** $W_{BSA} = 6$, **d** $W_{BSA} = 9$. The *arrows* shows the complex particle

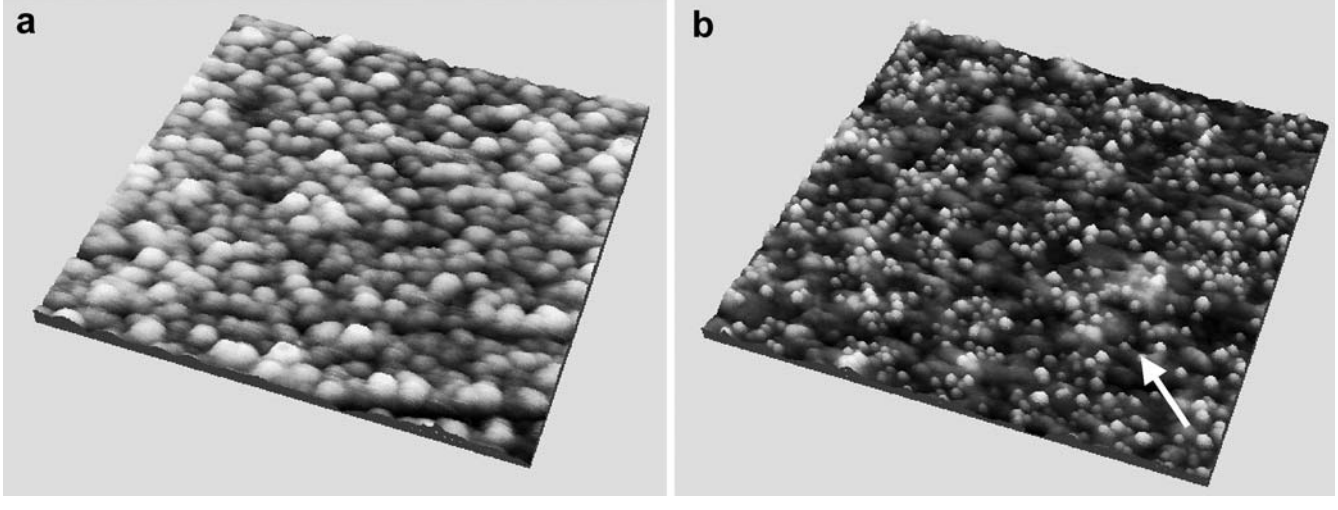

Fig. 7a,b Three-dimensional plots of a PMLG film and an unsaturated adsorption layer of a NaHA–BSA complex. **a** PMLG film, **b** NaHA–BSA complex (weight ratios of BSA to NaHA $W_{BSA} = 9$, degree of occupation $\theta = 0.6$). The *arrow* shows the complex particle

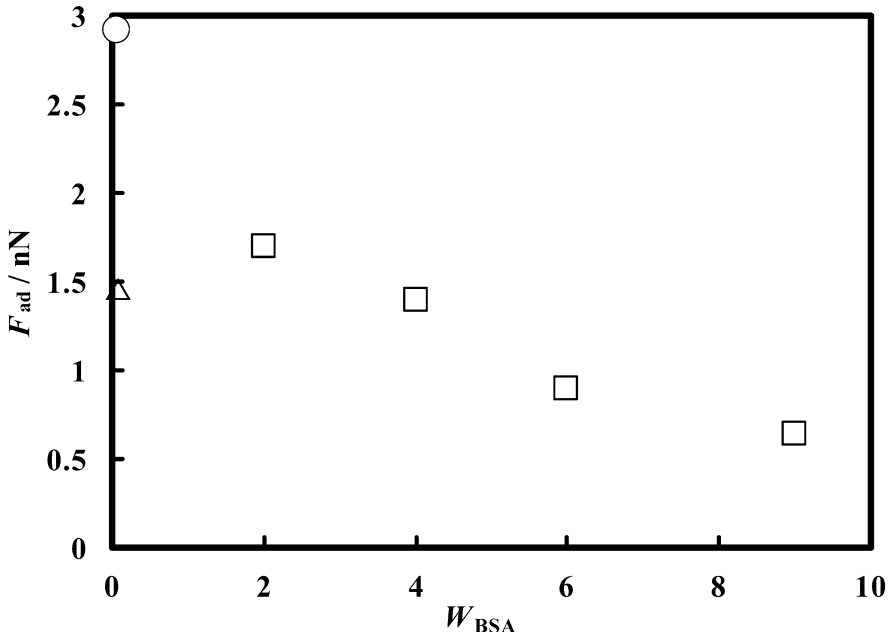

Fig. 8 Adhesion forces F_{ad} between NaHA–BSA complex layers and the AFM tip against weight ratios of BSA to NaHA. NaHA–BSA complex (*squares*), NaHA adsorption layer on a BSA monolayer (*circles*), PMLG film (*triangles*)

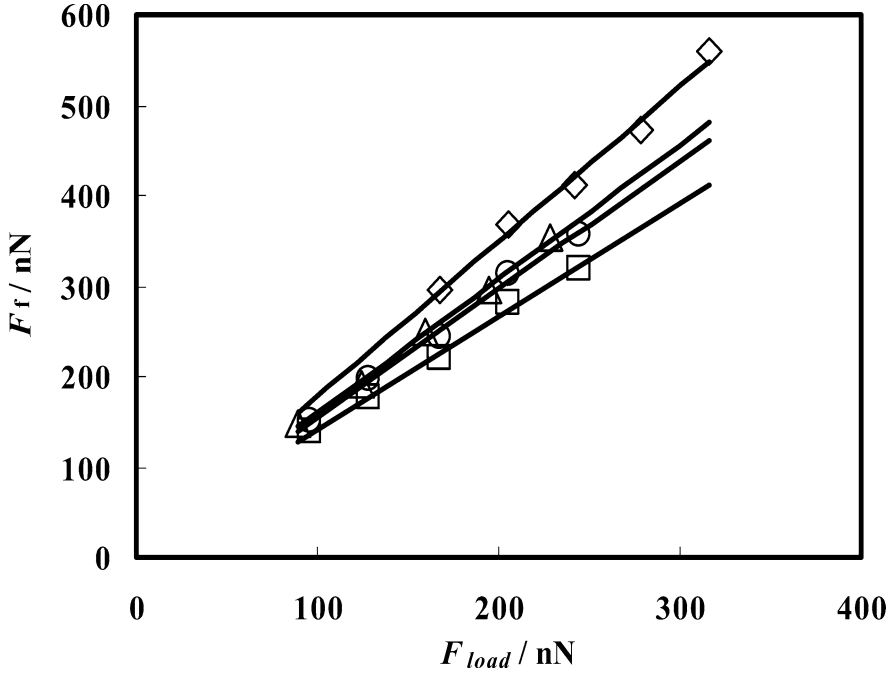

Fig. 9 Frictional forces F_f between a saturated adsorption layer of a NaHA–BSA complex and the AFM tip plotted against the load force exerted by a cantilever F_{load} in various weight ratios of BSA to NaHA $W_{BSA}=2$ (*squares*), $W_{BSA}=4$ (*circles*), $W_{BSA}=6$ (*triangles*), $W_{BSA}=9$ (*diamonds*)

Discussion

Adsorptions of NaHA–BSA complexes and structural transformation

The NaHA molecule possessing carboxylic groups is a rodlike or a wormlike structure in the neutral pH region owing to electrostatical repulsion and the stiffness of consecutive sugar rings. Adding BSA to NaHA solutions in the neutral and weakly acidic pH regions results in complexes being formed by electrostatical interaction. As shown in a previous paper [17], we reported that their complexes were formed in the solutions, which were the same ones as used in this study. In the region of $W_{BSA}<9$, soluble complexes were formed by an intramolecular association and free

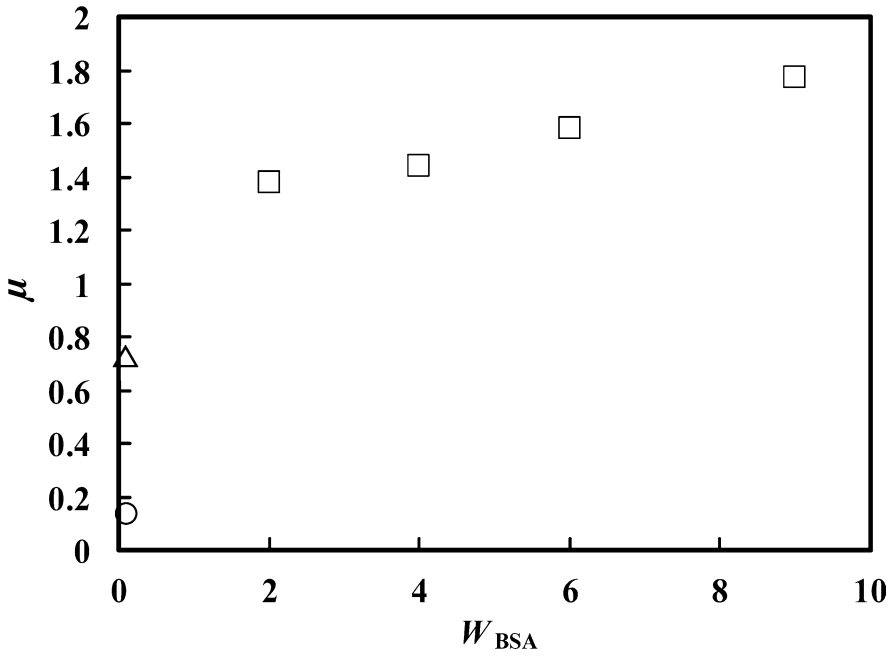

Fig. 10 Frictional coefficient μ between a saturated adsorption layer of a NaHA–BSA complex and the AFM tip plotted against the weight ratios of BSA to NaHA in the complex. NaHA–BSA complex (*squares*), NaHA adsorption layer on a BSA monolayer (*circles*), PMLG film (*triangles*)

BSA molecules were confirmed to be negligible from the spectra obtained by electrophoretic light scattering. With increasing values of W_{BSA}, the hydrodynamic diameter of the NaHA–BSA complexes d_H decreased from 1 μm to 96 nm. The decrease of d_H was ascribed to a structural transformation of the NaHA–BSA complex. As reported previously [17], when W_{BSA} increased, the structure of the NaHA–BSA complex transformed from a wormlike to a random-coil structure owing to intramolecular interactions between NaHA and BSA. Although the complex solutions were diluted in these adsorption studies, it is assumed that the compositions of the soluble complexes would remain unchanged and the values of d_H were almost the same as the original ones. Compared with the values of d_{AFM}, the values of d_H were much larger. From these results, it could be concluded that when the complexes adsorbed on the PMLG film, they were found to change their structures and shrank. Especially, the shrinkage became significant with decreasing W_{BSA}.

NaHA molecules could not adsorb on the PMLG film as shown in Fig. 1. On the other hand, BSA molecules adsorb on it owing to a physical interaction [1]. The adsorption of NaHA–BSA complexes on the PMLG film is ascribed to the interaction between BSA of the complexes and PMLG. Then, with increasing W_{BSA}, the affinities between the complexes and the PMLG film should increase. Furthermore, as the sizes in the solutions decreased with increasing W_{BSA}, the values of Γ and K are expected to increase. However, the values of K decreased with increasing W_{BSA}. The decrease of K is considered to result from the immobilization of BSA molecules in the complexes.

F_{ad} of NaHA–BSA complex adsorption layers

As shown in Fig. 8, with decreasing W_{BSA}, the values of F_{ad} of the NaHA–BSA complexes increased and approached that of the saturated adsorbed layer of NaHA on the BSA monolayer which was reported in a previous paper [19, 20]. The values of F_{ad} were obtained from the force–distance curves between the complexes and the AFM tip. As the AFM tip was located on an arbitrary complex, the values of F_{ad} would reflect the surface properties of the complex itself. Then, with decreasing W_{BSA}, the resulting F_{ad} is considered to approach the value of the NaHA adsorption layer.

As reported in a previous paper [17], the surface charges of the complexes were estimated to be negative and to approach zero with increasing W_{BSA} from their electrophoretic mobilities. The AFM tip composed of silicone nitrate also has a negative charge in our experimental conditions. Then, F_{ad} can be ascribed to non-electrostatical interactions between the complexes and the AFM tip.

μ of NaHA–BSA complex adsorption layers

It is known the frictional forces of a polymer film are affected not only by its surface morphology but also by its surface properties such as surface energy, rigidity and viscoelasticity. As frictional forces were obtained from the differences of the tip torsions in the scans of the trace and the retrace, the effects of the local morphology are cancelled out. The surface energy is related to F_{ad}. As the values of F_{ad} of the complexes were very small, the

effects of the surface energy would be very small. Then, the rigidity and the viscoelasticity of the surface play important roles in the frictional properties. With increasing W_{BSA}, the complex particles decreased slightly in diameter and the adsorption masses increased. So, we can consider that with increasing W_{BSA}, the densities of the complex increased, and as a result the rigidity and the viscoelasticity increased, which were attributed to the increases of μ. The values of μ were averaged over the scanning area. As the adsorption masses decreased with decreasing W_{BSA}, the values of μ are considered to approach that of the PMLG film. Furthermore, it should be noted that the values of μ of the NaHA–BSA complexes were much higher than that of the NaHA layer. Increases of μ due to the adsorption of the complexes are considered to relate to aging of a joint as well as to the decreases of M_w of NaHA [19].

Acknowledgements This research was supported by a grant from the Japan Society for the Promotion of Science (no. P 02183) and the Japan Health Sciences Foundation. Our thanks are extended to Seikagaku Kogyo Co. for supplying NaHA samples.

References

1. Nonogaki T, Xu S, Kugimiya S, Sato S, Miyata I, Yonese M (2000) Langmuir 16:4272
2. Vercruysse KD, Prestwich GD (1998) Crit Rev Ther Drug Carrier Syst 15: 513
3. Prestwich GD, Vercruysse KD (1998) Pharm Sci Technol Today 1:42
4. Luo Y, Ziebell MR, Prestwich GD (2000) Biomacromolecules 1:208
5. Meyer K, Palmer JW (1934) J Biol Chem 107:629
6. Weissman B, Meyer K (1954) J Am Chem Soc 76:1753
7. Sakamoto T, Mizuno S, Maki T, Suzuki T, Yamaguchi T, Iwata H (1984) Jpn Orthop Res Sci 11:264
8. Liesegang T J (1990) Surv Ophthalmol 34:268
9. Miyauchi S, Iwata S (1986) J Ocul Pharmacol 2:267
10. Kokufuta E, Dubin PL (1994) Surface 32:460 (in Japanese)
11. Xia JL, Dubin PL, Kim Y, Muhoberac BB, Klimkowski VJ (1993) J Phys Chem 97:4528
12. Tsuboi A, Izumi T, Hirata M, Xia JL, Dubin PL, Kokufuta E (1996) Langmuir 12:6295
13. Park JM, Muhoberac BB, Dubin PL, Xia J (1992) Macromolecules 25:290
14. Nishikawa T, Akiyoshi K, Sunamoto J (1996) J Am Chem Soc 118:6110
15. Nishikawa T, Akiyoshi K, Sunamoto J (1994) Macromolecules 27:7654
16. Yonese M, Xu S, Kugimiya S, Sato S, Miyata I (1997) Prog Colloid Polym Sci 106:252
17. Xu S, Yamanaka J, Sato S, Miyata I, Yonese M (2000) Chem Pharm Bull 48:779
18. Ge S, Kojio K, Takara A, Kajiyama T (1998) J Biomater Sci Polym Ed 9:131
19. Xu S, Sato S, Miyata I, Yamanaka J, Yonese M (2003) Mol Simul 29:1
20. Xu S, Yamanaka J, Sato S, Miyata I, Yonese M (2004) Colloid Polym Sci 282:440
21. Hara M, Higuchi M, Minoura N, Ohuchi S, Cho CS, Akaike T, Higuchi A (1996) Nippon Kagaku Kaishi 5:483
22. Okahata Y, Kimura K, Ariga K (1989) J Am Chem Soc 111:9190
23. Masuda H, Baba N (1990) Surface 28:222 (in Japanese)